

Localized bases of eigensubspaces and operator compression

Weinan E^a, Tiejun Li^{b,1}, and Jianfeng Lu^c

^aDepartment of Mathematics and Program in Applied and Computational Mathematics, Princeton University, Princeton, NJ 08544; ^bLaboratory of Mathematics and Applied Mathematics, and School of Mathematical Sciences, Peking University, Beijing 100871, China; and ^cProgram in Applied and Computational Mathematics, Princeton University, Princeton, NJ 08544

Communicated by Ingrid Daubechies, Princeton University, Princeton, NJ, November 24, 2009 (received for review November 21, 2007)

Given a complex local operator, such as the generator of a Markov chain on a large network, a differential operator, or a large sparse matrix that comes from the discretization of a differential operator, we would like to find its best finite dimensional approximation with a given dimension. The answer to this question is often given simply by the projection of the original operator to its eigensubspace of the given dimension that corresponds to the smallest or largest eigenvalues, depending on the setting. The representation of such subspaces, however, is far from being unique and our interest is to find the most localized bases for these subspaces. The reduced operator using these bases would have sparsity features similar to that of the original operator. We will discuss different ways of obtaining localized bases, and we will give an explicit characterization of the decay rate of these basis functions. We will also discuss efficient numerical algorithms for finding such basis functions and the reduced (or compressed) operator.

singular value decomposition | subspace iteration

Introduction

Given a local operator \mathcal{A} or a large sparse matrix A and a number M , it is well known that, in some appropriate sense, the $M \times M$ matrix that best approximates \mathcal{A} or A is its projection to the eigensubspaces corresponding to the M largest or smallest eigenvalues, depending on the problem. The question of interest in this paper is the following: Assuming that the operator \mathcal{A} is local or that the matrix A is sparse, how do we represent these subspaces most efficiently, i.e., how do we find basis vectors of these eigensubspaces that require the fewest degrees of freedom to represent?

Questions of this nature arise in many different contexts. Here are a few examples.

Low-Rank Approximation of a Large Matrix. In many applications ranging from DNA microarray analysis, facial and object recognition, to web search models, we encounter the following problem (1): Given a large $N \times N$ matrix A , one wants to find the best approximation of A by a low-rank matrix D , i.e.,

$$\min_{D \in \mathbb{R}^{N \times N}, \text{rank}(D) \leq k} \|A - D\|, \quad [1]$$

where the norm is usually taken as the spectral norm $\|\cdot\|_2$ or the Frobenius norm $\|\cdot\|_F$. The solution to this problem is easily formulated in terms of the singular value decomposition (SVD) of A . Finding it efficiently, however, is a nontrivial matter (1, 2).

Approximation of Differential Operators with Multiscale Coefficients. Consider an elliptic equation with multiscale coefficients:

$$-\nabla \cdot (a^\varepsilon(x) \nabla u^\varepsilon(x)) = f(x), \quad x \in D \subset \mathbb{R}^d, \quad [2]$$

$$u^\varepsilon(x) = 0, \quad x \in \partial D, \quad [3]$$

where D is a smooth domain in \mathbb{R}^d . Here, we used the notation $a^\varepsilon(x)$ to represent the coefficient to signal the fact that it varies

over many disparate scales. Our objective is to reduce this operator to an operator with fewer degrees of freedom or much less information content. When the scales of $a^\varepsilon(x)$ are far apart, this is a standard problem in homogenization theory, which tells us that the reduced operator takes the same form as in Eq. 2, except that the coefficient is replaced by the homogenized coefficient (3, 4). However, we are interested in the case when standard homogenization theory does not apply, i.e., when there is no particular structure in a^ε and, in particular, when there is no clear separation of scales. We will then ask the question: Given an integer M , what is the $M \times M$ matrix A_0 that best approximates the operator in Eq. 2.

Electronic Structure Analysis. The objective of electronic structure analysis using, for example, density functional theory, can be formulated as finding the eigensubspace of the Hamiltonian \mathcal{H} that corresponds to its lowest eigenvalues (5). This is a major problem in computational quantum chemistry and material science (6). Localized orbitals such as Wannier functions have been proposed, and it is expected that they will lead to the so-called linear scaling algorithms (7).

Reduction of Markov Chains on a Large Network. Many problems can be formulated as Markov chains on networks. Examples include chemical kinetic systems, diffusion and chemical reaction on surfaces, image processing, and, of course, dynamics on networks such as communication networks. Often such networks are rather large and it is of interest to reduce them to a much smaller state space. One classical idea is to lump the Markov chain (8). However, lumpability is a rather stringent condition which in many ways is analogous to the scale separation property discussed above for differential operators with multiscale coefficients. Just as the case the coefficients do not have separated scales, we should consider the situation when the Markov chain is not lumpable.

In principle, these problems can be considered as special cases of *model reduction*. In fact the solutions to these problems are given quite simply by different variants of SVD. However, the standard SVD algorithms have a complexity of $\mathcal{O}(M^2N)$. This is too costly when $M \gg 1$. In addition, the outputs of SVD are eigenvectors, which are global objects. This is sometimes not as convenient as local ones.

The viewpoint we will take is the following: Our real interest is the subspace itself, not the particular basis functions. Although the eigenvectors form a natural basis set, we are free to choose other basis sets which may better suit our purposes. In particular, for the problems discussed above, it is of special interest to choose a localized basis set. This will enable us to obtain sparse representation for the basis functions and the reduced operator. This philosophy is similar to that of the multiresolution analysis of operators (9), except that we are now dealing with a large

Author contributions: W.E., T.L., and J.L. designed research, performed research, contributed new reagents/analytic tools, analyzed data, and wrote the paper.

The authors declare no conflict of interest.

¹To whom correspondence should be addressed. E-mail: tieli@pku.edu.cn.

However, even in the general case, it is still possible that some features of translational invariance are retained. For example, we may expect that the functions ψ_j have similar shapes for different j . This is definitely not the case for the eigenbases.

Approximate δ -Functions. We can view the Dirichlet kernel as the projection of δ -function, which is the most localized function, to the subspace V_M : Let $\delta(x) = \sum_{k=-\infty}^{\infty} e^{ikx}$; its projection to V_M is

$$\delta_n(x) = D_n(x) = \sum_{k=-n}^n e^{ikx} = \frac{\sin(n + \frac{1}{2})x}{\sin \frac{x}{2}}, \quad -\pi \leq x \leq \pi$$

which is the Dirichlet kernel. The slow decay of the oscillatory tail of D_n is a result of the Gibbs phenomenon caused by the lack of smoothness of $\delta(x)$. An obvious idea for obtaining basis functions with better decay properties is to use filtering (20). We define

$$\delta_n^\sigma(x) = \sum_{k=-n}^n \sigma\left(\frac{k}{n}\right) e^{ikx}, \quad [11]$$

where $\sigma(\eta)$ is a filter. The decay properties of δ_n^σ depends on the smoothness of the filter σ . The following result is well known.

Lemma 1. Assume that σ satisfies the following conditions for positive integer p :

1. $\sigma(\eta)$ is real and even in $(-\infty, +\infty)$.
2. $\sigma(0) = 1$, and if $p \geq 2$, $\sigma^{(l)}(0) = 0$, $1 \leq l \leq p - 1$.
3. $\sigma(\eta) = 0$, $|\eta| \geq 1$.
4. $\sigma(\eta) \in C^{p-1}(\mathbb{R})$ and $\sigma^{(p)}(\eta) \in BV(\mathbb{R})$.

Then we have

$$\left| \frac{1}{n} \delta_n^\sigma(x) \right| \leq C \frac{1}{|nx|^{p+1}} \|\sigma^{(p)}\|_{BV}, \quad x \in (-\pi, \pi), x \neq 0, \quad [12]$$

where C is a constant independent of n and x , $\|\cdot\|_{BV}$ is the bounded variation norm.

The filter $\sigma(\eta)$ satisfying the above conditions is called a p th-order filter (20). The Dirichlet kernel corresponds to the case when $\sigma(\eta) = \chi_{[-1,1]}(\eta)$, which is a zeroth-order filter in the sense of [12]. If we take $\sigma(\eta) = 1 - |\eta|$ ($\eta \in [-1, 1]$), which is a first-order filter, we obtain the Fejér kernel.

If we use the filtered kernel to form the basis functions, the components of the compressed operator for the Laplacian can be found as follows:

$$A_0 = \left(\sum_{l=-n}^n l^2 \sigma^2\left(\frac{l}{n}\right) \cos \frac{2l(j-k)\pi}{2n+1} \right)_{j,k=1}^M \quad [13]$$

up to a normalization constant. The behavior of A_0 is similar to that shown in Fig. 2, i.e., the entries decay away from the diagonal. More results on the basis functions that correspond to the filtered delta functions can be obtained similarly from Eq. 11.

Localization Using Weight Function. Another natural idea for obtaining localized bases is to use a weight function. More precisely, consider the following variational problem:

$$\min_{\psi \in V_M, \psi \neq 0} \mathcal{B}[\psi] = \frac{\int_{-\pi}^{\pi} w(x) |\psi(x)|^2 dx}{\int_{-\pi}^{\pi} |\psi(x)|^2 dx}, \quad [14]$$

where the weight function $w(x)$ is an even, nonnegative periodic function in $[-\pi, \pi]$ with $w(0) = 0$. Such ideas have been explored in ref. 21 for electronic structure computation where $w(x) = x^2$ is used.

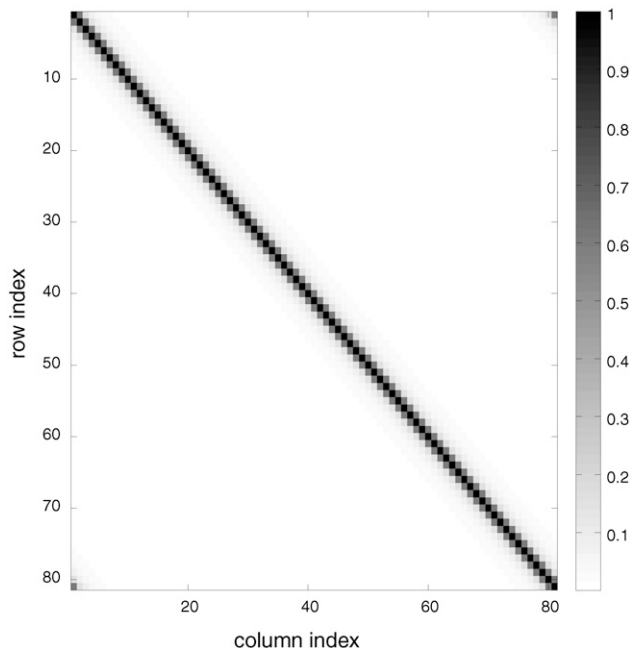


Fig. 2. Gray map of the magnitude of the entries of the compressed matrix A_0 .

The minimization problem [14] is equivalent to an eigenvalue problem

$$Bc = \lambda_{\min} c, \quad B \in \mathbb{R}^{M \times M}, \quad [15]$$

where $\psi(x) = \sum_{j=1}^M c_j \psi_j(x)$, $\{\psi_j(x)\}_{j=1}^M$ are the eigenbases, and the matrix

$$B = \left(\int_{-\pi}^{\pi} w(x) \overline{\psi_j(x)} \psi_k(x) dx \right)_{j,k=1}^M.$$

The smallest eigenvalue of B is λ_{\min} .

Take the Laplace operator as an example: Let $M = 2n + 1$, $\psi_j(x) = e^{ijx}$, $j = -n, -n + 1, \dots, n$, using the weight function x^2 , we obtain the localized bases shown in Fig. 3. It is easy to see that these basis functions decay faster than the Dirichlet kernel.

The eigenvalue problem [15] can be expressed in a more explicit form. Assume that the weight function has the Fourier representation $w(x) = \sum_{j=-\infty}^{\infty} w_j e^{ijx}$, $w_j = w_{-j} \in \mathbb{R}$ since $w(x)$ is real and even, [14] is equivalent to

$$\mathcal{P}_M(w(x)\psi(x)) = \lambda_{\min} \psi(x), \quad \psi(x) \in V_M, \quad [16]$$

where \mathcal{P}_M is the projection operator to the subspace V_M . The eigenvalue problem then becomes

$$Wc = \lambda_{\min} c, \quad [17]$$

where

$$W = (w_{j-k})_{j,k=0}^{2n}, \quad c = (c_j)_{j=-n}^n. \quad [18]$$

Note that W is a real symmetric Toeplitz matrix (22).

It is natural to ask whether we can obtain a characterization for basis functions obtained using weight functions. To answer this question, we will find an effective filter for a given weight function, when applied to the example V_M . If we set $\sigma_n(\frac{k}{n}) = c_k$, we have

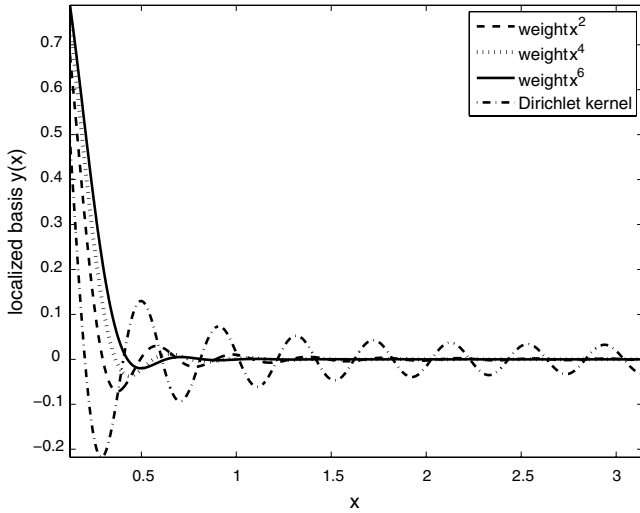


Fig. 3. Localized bases produced by the weight functions x^2 (dashed curve), x^4 (dotted curve), and x^6 (solid curve) and the Dirichlet kernel with $n = 16$ (dot-dashed curve). Here, the best localization is obtained with the weight function x^6 .

$$\psi(x) = \sum_{k=-n}^n c_k e^{ikx} = \sum_{k=-n}^n \sigma_n \left(\frac{k}{n} \right) e^{ikx} = \delta_n^{\sigma_n}(x). \quad [19]$$

Assuming that, as $M \rightarrow \infty$, σ_n has a limit σ , the localized function obtained by minimizing [14] can then be regarded as an approximation of δ -function with filter σ . This observation suggests considering the limiting problem of [16] and [17].

Assume that c is given by $c_k = \sigma \left(\frac{k}{n} \right)$, where σ is smooth and equal to zero outside $(-1, 1)$. The key is to understand the behavior of Wc as $M \rightarrow \infty$, where W is defined as in Eq. 18. In this direction, we have

Lemma 2. Assume that the weight function w is smooth in $(-\pi, \pi)$. If $w^{(2l)}(0)$ is the first nonzero term in $\{w^{(2m)}(0) | m \in \mathbb{N}\}$, we have

$$n^{2l} Wc \rightarrow \mathcal{L}\sigma, \quad [20]$$

pointwise as $M \rightarrow \infty$, where $\mathcal{L} = \frac{1}{(2l)!} w^{(2l)}(0) (-\Delta)^l$.

According to Lemma 2, only the local behavior of w at the origin matters in the limit. This is easy to understand intuitively because, as M becomes large, the basis function becomes more localized around zero, and hence it only feels the local behavior of w there.

Proof: The proof of Lemma 2 is based on the observation that W can be regarded as the discretization of a differential operator. Because zero boundary condition is assumed,

$$(Wc) \left(\frac{k}{n} \right) = \sum_j w_j \sigma \left(\frac{k-j}{n} \right).$$

Taylor expand σ around $\frac{k}{n}$, we get

$$\begin{aligned} (Wc) \left(\frac{k}{n} \right) &= \sum_j w_j \left(\sum_{m=0}^{\infty} \frac{1}{(2m)!} \sigma^{(2m)} \left(\frac{k}{n} \right) \left(\frac{j}{n} \right)^{2m} \right) \\ &= \sum_{m=0}^{\infty} \frac{1}{(2m)! n^{2m}} \left(\sum_j w_j j^{2m} \right) \sigma^{(2m)} \left(\frac{k}{n} \right) \end{aligned}$$

because the odd order terms vanish due to the symmetry of w_j . An elementary computation gives

$$\sum_{j=-2n}^{2n} w_j j^{2m} = (-1)^m \int_{-\pi}^{\pi} w^{(2m)}(x) \sum_{j=-2n}^{2n} e^{-ijx} dx \rightarrow (-1)^m w^{(2m)}(0),$$

as M and hence n goes to infinity. Assume that $w^{(2l)}(0)$ is the first nonzero term in $\{w^{(2m)}(0) | m \in \mathbb{N}\}$, it is clear that

$$n^{2l} (Wc)(x) \rightarrow (-1)^l \frac{1}{(2l)!} w^{(2l)}(0) \sigma^{(2m)} \left(\frac{k}{n} \right) = \mathcal{L}\sigma(x)$$

by the definition of \mathcal{L} .

Given the weight function w , the effective filter is characterized by the problem

$$\frac{1}{(2l)!} w^{(2l)}(0) (-\Delta)^l \sigma = \lambda_{\min} \sigma, \quad [21]$$

$$\sigma^{(k)}(\pm 1) = 0, \quad k = 0, 1, \dots, l-1. \quad [22]$$

The smoothness of σ improves as l increases. The effective filter functions can be found by solving the eigenvalue problems [21] and [22]. For $w(x) = x^2$, the effective filter function is given explicitly by $\sigma(\eta) = \cos(\pi\eta/2)$. The different effective filter functions corresponding to the weight functions x^2 and x^6 are shown in Fig. 4. Putting Lemma 1 and Lemma 2 together, we arrive at

Corollary 1. Assume that w is smooth in $(-\pi, \pi)$. If $w^{(2l)}(0)$ is the first nonzero term in $\{w^{(2m)}(0) | m \in \mathbb{N}\}$, then

$$\left| \frac{1}{n} \psi(x) \right| \leq \frac{C}{nx^{l+1}}, \quad x \in (-\pi, \pi), x \neq 0, \quad [23]$$

where C is a constant independent of n and x .

The basis functions produced with the weight functions x^2 , x^4 and x^6 are shown in Fig. 3. Only one basis function is shown for each case, due to the translation invariance property.

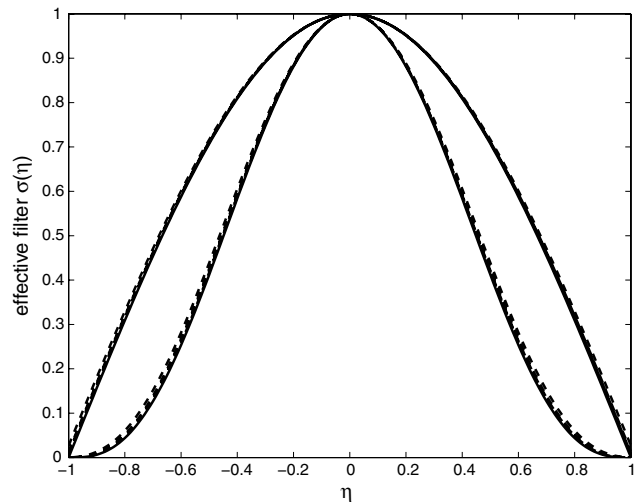


Fig. 4. Comparison between the effective filter function in the limit $n \rightarrow \infty$ (solid curve) and the numerical filter functions for large n ($n = 50$ and 200) (dashed curve). The upper and lower curves are the effective filters with weight functions x^2 and x^6 , respectively. The lower curve is smoother.

Remark 1: Another interesting weight function is proposed in (23): $w(x) = 1 - \chi_{[-R_c, R_c]}$, where R_c is the localization radius and χ is the characteristic function.

Remark 2: Corollary 1 suggests choosing $w(x) = x^{2l}$ with large l . However, this is only part of the story. The other important part of the story is numerical stability, i.e., condition number of the system. It can be shown that the condition number increases like $O((\pi/\varepsilon_M)^l)$, where ε_M is the minimal eigenvalue of W in the space V_M . Therefore, the best weight function has to be a compromise between smoothness and numerical stability. Numerical results show the weight functions x^6 and x^8 are good choices.

Remark 3: Given a weight function, Lemma 2 tells us how to find the effective filter. It is natural to consider the inverse problem: Given a filter σ , can we find a weight function w that corresponds to this filter? This problem is closely related to the inverse Toeplitz eigenvalue problem, which is quite nontrivial. Some existence results are proved by Landau in ref. 24.

Results

In the general case, we will have to resort to numerical computations to find the bases discussed above. The standard numerical technique for finding eigensubspaces is the subspace iteration method (25, 26). This is a generalization of the power method for computing leading eigenvalues and eigenvectors of a matrix. Subspace iteration consists of two main steps: multiplication of a set of approximate basis vectors by the matrix A and orthogonalization (25, 26). We propose a localized version of this algorithm, in which the orthogonalization step is replaced by a localization step. The resulting algorithm has a complexity of $O(N)$ instead of $O(N + M^3)$.

To begin with, we choose beforehand the localization regions $\{S_i\}_{i=1}^M$ which will be the support of the basis functions and the weight functions $\{w_i\}_{i=1}^M$ centered in S_i , which are appropriate translations of the weight function analyzed above. The choice of these regions will have to be informed by the understanding of the specific problems. Adaptive algorithms for choosing these sets can be contemplated but have not yet been investigated.

Algorithm 1 (Localized Subspace Iteration). Knowing $\{Q_i^{(n)}\}$, we find $\{Q_i^{(n+1)}\}$ by the following steps:

1. Purification: Compute $\tilde{Q}_i^{(n+1)} = p(A)Q_i^{(n)}$, $i = 1, 2, \dots, M$;
2. Localization: For each $i = 1, 2, \dots, M$, denote by $V_i = \text{span}\{\tilde{Q}_j^{(n+1)}\}$ the linear space spanned by $\tilde{Q}_j^{(n+1)}$ whose support overlaps with that of $\tilde{Q}_i^{(n+1)}$. Find $\hat{Q}_i^{(n+1)}$ in V_i by solving the variational problem

$$\min_{\hat{Q}_i^{(n+1)} \in V_i, \|\hat{Q}_i^{(n+1)}\|_{2, w_i} = 1} \|\hat{Q}_i^{(n+1)}\|_{2, w_i}. \quad [24]$$

Here, $\|\cdot\|_{2, w_i}$ is the weighted l^2 norm with weight function w_i .

3. Truncation: $Q_i^{(n+1)}$ is the truncation of $\hat{Q}_i^{(n+1)}$ on S_i ,

$$Q_i^{(n+1)} = \hat{Q}_i^{(n+1)} \chi_{S_i}, \quad [25]$$

where χ_{S_i} is the indicator function of S_i .

In the algorithm, $p(A)$ is some polynomial. A good choice is the Chebyshev polynomial (26). For an illustration of the algorithm and the resulting localized bases, we consider a differential operator with ε -periodic coefficient: $A = -\nabla \cdot (a(x/\varepsilon)\nabla)$ with $a(y) = 1 + 0.5 \cos(2\pi y)$ on the interval $[0, 21]$ with periodic boundary condition. We take $M = 21$ and therefore the corresponding coarse grid size is one. The small parameter ε is chosen to be one-eighth and the operator is discretized with standard second-order finite difference scheme with fine grid size $1/64$.

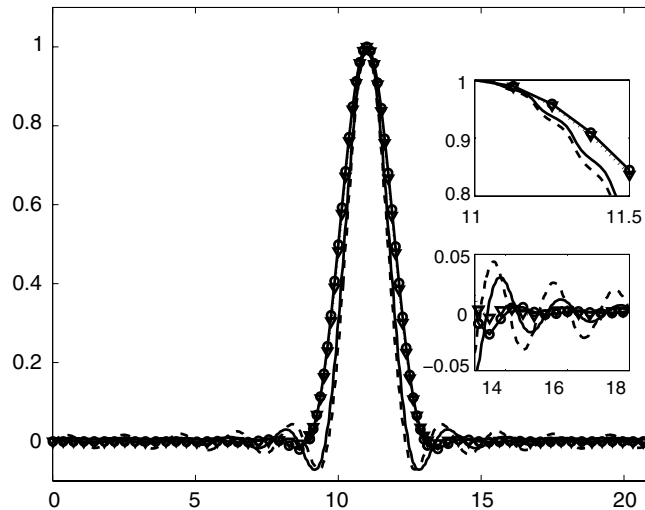


Fig. 5. Homogenization problem: The localized bases produced by the weight functions x^2 (solid curve), x^6 (circle-solid curve), $1 - \chi_{[-1,1]}$ (dashed curve), and $1 - \chi_{[-2,2]}$ (triangle-dotted curve). The bottom inset shows the tail region, whereas the top inset shows the oscillatory behavior of the basis functions in more detail.

Four weight functions are used: x^2 , x^6 , $1 - \chi_{[-R_c, R_c]}$ with $R_c = 1$, and 2; the resulting localized bases are shown in Fig. 5. In Fig. 6, we compare the localized bases with the basis function from the generalized finite element method (15, 17) with support sizes two and four (corresponding to the choices $R_c = 1$ and 2, respectively). One can see that the generalized (or multiscale) finite element basis with support size four compares much better with the bases produced using our approach. Detailed results on the application of the ideas presented here to homogenization problems can be found in ref. 14.

Other applications of the algorithm include electronic structure calculation (12) and image segmentation (13). Some issues of accuracy and convergence in the context of electronic structure calculation are discussed in ref. 27.

Discussion

There is a long list of problems that need to be investigated further. On the algorithmic side, the most pressing problem is

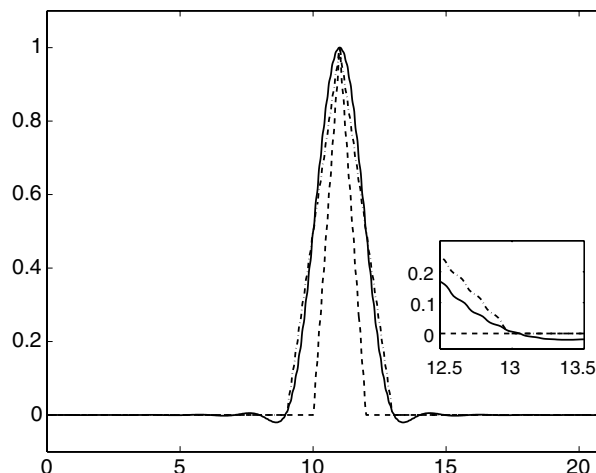


Fig. 6. Homogenization problem: The localized bases produced by the weight functions x^6 (solid curve) compared with the basis function of the generalized finite element method (or MsFEM) with support size two (dashed curve) and four (dashed-dot curve). The inset shows the detail of these basis functions two coarse grids away from the center.

to speed up the convergence of the algorithms discussed here. On the numerical analysis side, it is crucial that we have a clear understanding of the effect of truncating the support of the basis functions. Of course, the application of these ideas remains largely unexplored, although initial progress has been made for some of the problems discussed in the Introduction.

ACKNOWLEDGMENTS. W.E. and J.L. are supported in part by Office of Naval Research Grant N00014-01-0674, Department of Energy Grant DE-FG02-03ER25587, and National Science Foundation Grant DMS0708026. T.L. is partially supported by National Science Foundation of China under Grant 10401004 and the National Basic Research Program under Grant 2005CB321704.

1. Drineas P, Kannan R, Mahoney W (2006) Fast Monte Carlo algorithms for matrices II: Computing a low-rank approximation to a matrix. *SIAM J Comput*, 36:158–183.
2. Koch O, Lubich C (2007) Dynamical low rank approximation. *SIAM J Matrix Anal A*, 29:434–454.
3. Bensoussan A, Lions JL, Papanicolaou G (1978) *Asymptotic Analysis for Periodic Structures* (North-Holland, Amsterdam).
4. Zhikov VV, Kozlov SM, Oleinik OA (1994) *Homogenization of Differential Operators and Integral Functionals* (Springer-Verlag, Berlin).
5. E W (2007) *Sixth International Congress on Industrial and Applied Mathematics*, ed Jeltsch R (EMS Publishing House, Zürich), pp 113–130.
6. Martin R (2004) *Electronic Structure: Basic Theory and Practical Methods* (Cambridge Univ. Press, Cambridge, UK).
7. Goedecker S (1999) Linear scaling electronic structure methods. *Rev Mod Phys*, 71:1085–1123.
8. Kemeny JG, Snell JL (1960) *Finite Markov chains* (Van Nostrand, New York).
9. Belykin G, Coifman R, Rokhlin V (1991) Fast wavelet transforms and numerical algorithms I. *Commun Pure Appl Math*, 44:141–183.
10. Kohn W (1959) Analytic properties of Bloch waves and Wannier functions. *Phys Rev*, 115:809–821.
11. Wannier GH (1937) The structure of electronic excitation levels in insulating crystals. *Phys Rev*, 52:191–197.
12. García-Cervera CJ, Lu J, E W (2007) A sub-linear scaling algorithm for computing the electronic structure of materials. *Commun Math Sci*, 5:999–1026.
13. Wu J, Li T (2008) Image segmentation by using the localized subspace iteration algorithm. *Sci China Ser A*, 51:1495–1509.
14. Dorobantu M, Engquist B (1998) Wavelet-based numerical homogenization. *SIAM J Numer Anal*, 35:540–559.
15. Babuška I, Osborn JE (1983) Generalized finite element methods: their performance and their relation to mixed methods. *SIAM J Numer Anal*, 20:510–536.
16. Wan WL, Chan TF, Smith B (1999) An energy-minimizing interpolation for robust multigrid methods. *SIAM J Sci Comput*, 21:1632–1649.
17. Hou TY, Wu X (1997) A multiscale finite element method for elliptic problems in composite materials and porous media. *J Comput Phys*, 134:169–189.
18. Xu J, Zikatanov L (2004) On an energy minimizing basis for algebraic multigrid methods. *Comput Visual Sci*, 7:121–127.
19. Zygmund A (1959) *Trigonometric series* (Cambridge Univ. Press, New York), 2nd Ed.
20. Gottlieb D, Shu CW (1997) On the Gibbs phenomenon and its resolution. *SIAM Rev*, 39:644–668.
21. Marzari N, Vanderbilt D (1997) Maximally localized generalized Wannier functions for composite energy bands. *Phys Rev B*, 56:12847–12865.
22. Gray RM (2006) *Toeplitz and Circulant Matrices: A Review* (Now Publishers, Norwell, MA).
23. Gao W, E W (2009) Orbital minimization with localization. *Discret Contin Dyn Sys*, 23:249–264.
24. Landau HJ (1994) The inverse eigenvalue problem for real symmetric Toeplitz matrices. *J Am Math Soc*, 7:749–767.
25. Golub G, Van Loan C (1996) *Matrix Computation* (The Johns Hopkins Univ Press, Baltimore).
26. Saad Y (1992) *Numerical Methods for Large Eigenvalue Problems* (Manchester Univ. Press, Manchester, UK).
27. García-Cervera CJ, Lu J, Xuan Y, E W (2009) A linear scaling subspace iteration algorithm with optimally localized non-orthogonal wave functions for Kohn-Sham density functional theory. *Phys Rev B*, 79:115110–2009.